COLLISION, DAMAGE, SMOOTH EVOLUTION OF AN ARTICULATION. THE "TENNIS ELBOW"

FRANCESCO BONALDI AND MICHEL FRÉMOND

Abstract. We present a simple example of phenomenon where collision and damage take place together. We consider an arm with its forearm connected by the elbow: a plane system made of two rods, one of which is clamped and the other is hinged at its extremum and free to rotate about it. The rotation angle ϑ of the forearm is constrained to be neither larger than π nor lower than 0. The rods are connected through a hair spring, which represents the elbow articulation and whose damage is accounted for. The damage may be related to the tennis elbow pathology. We also take into account the discontinuity of the angular velocity of the forearm, due to collisions when $\vartheta = 0$ or $\vartheta = \pi$, and provide some numerical results.

Sommario. Presentiamo un semplice esempio di fenomeno in cui intervengono insieme sia urto che danno. Consideriamo un braccio con il suo avambraccio connesso mediante il gomito: un sistema piano composto di due aste, la prima bloccata, la seconda incernierata alla prima in un suo estremo e libera di ruotare attorno ad esso. L'angolo di rotazione ϑ dell'avambraccio è vincolato ad essere compreso tra 0 e π. Le aste sono connesse tramite una molla rotazionale, che rappresenta l'articolazione del gomito e di cui si tiene conto del danno. Il danno può essere legato alla patologia del "gomito del tennista". Teniamo conto anche della discontinuità della velocità angolare dell'avambraccio, dovuta agli urti quando $\vartheta = 0$ o $\vartheta = \pi$, e forniamo alcuni risultati numerici.

1. Introduction

Let us consider the system represented in fig. 1. It is a schematic representation of an arm with its forearm connected by the elbow. Its only degree of freedom is the elbow opening $\vartheta \in [0, \pi]$. We suppose the elbow articulation to act as a hair spring with elastic constant k. The tennis elbow pathology is caused by repetitive activities, such as hitting thousands and thousands of tennis balls, or lifting movements, which lead to tiny tears in the forearm tendon attachment at the elbow. Thus, we take into account the *damage* of the articulation through a quantity $\beta \in [0, 1]$.

More detailed biological description of the arm system is given in [1, 2, 3]. It involves modelling of the smooth and non-smooth motion without damage.

We say that the articulation is sound when $\beta = 1$, partly broken when $0 < \beta < 1$ and completely broken when $\beta = 0$ [4, 5]. An external torque C is applied to the system and our aim is to predict its evolution in terms of the mappings $t \mapsto \vartheta(t)$ and $t \mapsto \beta(t)$. Let us

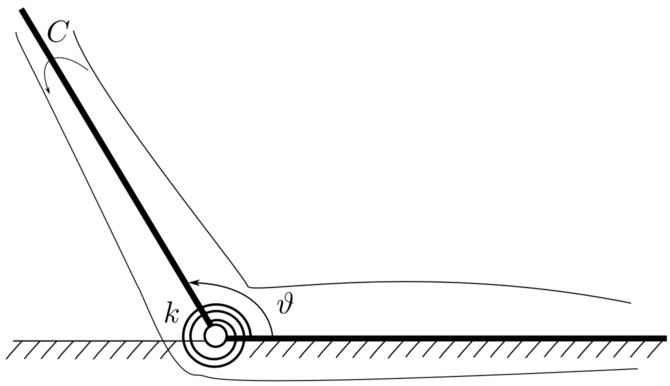

FIGURE 1. The “tennis elbow”.

note that there may be discontinuities of the angular velocity due to collisions when $\vartheta = 0$ or $\vartheta = \pi$.

2. Smooth evolution

2.1. **Equations of motion.** In order to get the equations of motion, we apply the Principle of Virtual Power (PVP) [4, 6]. The *actual* powers are:

$$\mathcal{P}_{acc}(\dot{\vartheta}, \dot{\beta}) = J\ddot{\vartheta}\,\dot{\vartheta},$$
$$\mathcal{P}_{int}(\dot{\vartheta}, \dot{\beta}) = -\left(C^{int}\dot{\vartheta} + B^{int}\dot{\beta}\right),$$
$$\mathcal{P}_{ext}(\dot{\vartheta}, \dot{\beta}) = C\dot{\vartheta} + A\dot{\beta},$$

where J is the mass moment of inertia of the system, A is an external damaging work, C is the external torque (which is assumed to be a smooth function of time), B^{int} is an internal damaging work which takes into account the effect of the damage velocity and C^{int} is a torque which accounts for the action of the hair spring on the forearm. If ω and δ are, respectively, the *virtual* angular velocity and the *virtual* damage velocity, the PVP reads

$$\forall \omega, \delta \in \mathbb{R}, \quad \mathcal{P}_{acc}(\omega, \delta) = \mathcal{P}_{int}(\omega, \delta) + \mathcal{P}_{ext}(\omega, \delta).$$

By fixing $\delta = 0$, we get

$$C - C^{int} = J\ddot{\vartheta}; \tag{1}$$

by fixing $\omega = 0$, we get

$$A - B^{int} = 0.$$

For the problem we are going to study, we assume $A = 0$, but either due to illness, aging, or overuse, there may be a biological source of damage $A \neq 0$. Thus, we have

$$B^{int} = 0. \tag{2}$$

2.2. **Constitutive laws.** In order to get constitutive laws for the internal quantities B^{int} and C^{int}, we need to choose a *free energy*, which takes into account the quantities at the equilibrium, and a *pseudopotential of dissipation*, which takes into account quantities which describe the evolution [4, 6]. Thus, we take

$$\Psi(\vartheta,\beta)=\frac{1}{2}k\beta\vartheta^2+w(1-\beta)+L(\vartheta)+I(\beta)$$

as free energy and

$$\Phi(\dot{\vartheta},\dot{\beta})=\frac{1}{2}c\dot{\beta}^2+\frac{1}{2}\nu\dot{\vartheta}^2+I_-(\dot{\beta})$$

as pseudopotential of dissipation, where k is the elastic constant of the hair spring, w the cohesion energy of the articulation, c the damage viscosity, ν the motion viscosity, I the indicator function[1] of $[0,1]$, I_- the indicator function of $(-\infty,0]$, L the indicator function of $[0,\pi]$ [7, 8]. These choices are due to the constraints on ϑ and β and to the condition of *irreversible* damage ($\dot{\beta}\le 0$). Thus, we obtain

$$\begin{aligned} C^{int}&=\frac{\partial\Psi}{\partial\vartheta}+\frac{\partial\Phi}{\partial\dot{\vartheta}}=k\beta\vartheta+\nu\dot{\vartheta}+C^r,\\ B^{int}&=\frac{\partial\Psi}{\partial\beta}+\frac{\partial\Phi}{\partial\dot{\beta}}=c\dot{\beta}+\frac{1}{2}k\vartheta^2-w+B^r, \end{aligned}\tag{3}$$

with $C^r\in\partial L(\vartheta)$, $B^r=B^{rnd}+B^{rd}$, $B^{rnd}\in\partial I(\beta)$ and $B^{rd}\in\partial I_-(\dot{\beta})$; C^r is the reactive torque, B^r is the reactive damaging-work which is split into its dissipative part B^{rd} and its non-dissipative part B^{rnd}. Here, $\partial f(x)$ denotes the subdifferential[2] of a convex function f at point x [7, 8]. Note that

$$C^r=\begin{cases}0 \text{ if } \vartheta\in(0,\pi)\\ \mathcal{C}^+ \text{ if } \vartheta=\pi\\ \mathcal{C}^- \text{ if } \vartheta=0, \qquad \mathcal{C}^+\ge 0,\ \mathcal{C}^-\le 0;\end{cases}$$

we have $C^r\in\emptyset$ if $\vartheta\notin[0,\pi]$, thus relationship $C^r\in\partial L(\vartheta)$ proves that $\vartheta\in[0,\pi]$. Moreover,

$$B^r=\begin{cases}0 \text{ if } \beta\in(0,1) \text{ and } \dot{\beta}<0\\ \mathcal{B} \text{ if } \beta=0 \text{ or } \beta=1 \text{ or } \dot{\beta}=0, \qquad \mathcal{B}\in\mathbb{R}\end{cases}$$

and we have $B^r\in\emptyset$ if either $\beta\notin[0,1]$ or $\dot{\beta}>0$, thus relationship $B^r\in\partial I(\beta)+\partial I_-(\dot{\beta})$ proves that $\beta\in[0,1]$ and $\dot{\beta}\le 0$. Therefore, C^r and B^r intervene only when the constraints

[1]The *indicator function* $I_C:\mathbb{R}^n\to\overline{\mathbb{R}}$, $\overline{\mathbb{R}}=\mathbb{R}\cup\{+\infty\}$, of a convex set $C\subset\mathbb{R}^n$ is defined by [7, 8]

$$I_C(x)=\begin{cases}0, & \text{if } x\in C,\\ +\infty, & \text{otherwise.}\end{cases}$$

[2]The *subdifferential* of a convex function $f:\mathbb{R}\to\overline{\mathbb{R}}$ at point x is the set [7, 8]

$$\partial f(x)=\{p\in\mathbb{R}: f(x)+p(y-x)\le f(y), \forall y\in\mathbb{R}\}.$$

on ϑ, β and $\dot\beta$ are going to be violated. By inserting the constitutive laws (3) into the equations of motion (1) and (2), we obtain the following nonlinear differential system in the unknowns $t \mapsto \vartheta(t)$ and $t \mapsto \beta(t)$:

$$
\begin{cases}
J\ddot\vartheta + \nu\dot\vartheta + k\beta\vartheta + C^r = C \\
c\dot\beta + B^r = w - \frac{1}{2}k\vartheta^2 \\
\vartheta(0) = \vartheta^0, \ \dot\vartheta(0) = \dot\vartheta^0 \\
\beta(0) = \beta^0.
\end{cases}
\tag{4}
$$

Remark 1. *Note that, from equation* $(4)_2$*, if* k *and* w *satisfy the inequality* $w - \frac{1}{2}k\pi^2 > 0$ *we never get damage, because the constraint* $\dot\beta \leq 0$ *would be violated for any* t*. On the other hand, we get damage for all* t *such that* $w - \frac{1}{2}k\vartheta^2(t) < 0 \iff \sqrt{\frac{2w}{k}} < \vartheta(t) < \pi$ *and no damage for all* t *such that* $w - \frac{1}{2}k\vartheta^2(t) > 0 \iff 0 < \vartheta(t) < \sqrt{\frac{2w}{k}}$.

Remark 2. *When* $\beta = 0$ *the system has lost its elasticity: it is still operating, but in a loose way.*

3. Non-smooth evolution

Because we have assumed the external torque C to be smooth, discontinuities of the angular velocity are only due to collisions of the forearm when $\vartheta = 0$ or $\vartheta = \pi$, and since the case of $\vartheta = 0$ is completely analogous, we analyse the collision only for $\vartheta = \pi$. We do not take into account discontinuities of the damage velocity.

3.1. Equation of motion.

Let $\Omega = \dot\vartheta$ be the angular velocity and t^* be a collision time, when either $\vartheta = \pi$ or $\vartheta = 0$. The angular velocity is discontinuous with

$$\Omega^- = \lim_{\Delta t \to 0^+} \Omega(t^* - \Delta t)$$

being the velocity before the collision, and

$$\Omega^+ = \lim_{\Delta t \to 0^+} \Omega(t^* + \Delta t)$$

being the velocity after the collision. The Principle of Virtual Work at collision time [9] is

$$\forall \hat\Omega \in \mathbb{R}, \quad J(\Omega^+ - \Omega^-)\hat\Omega = -P^{int}\hat\Omega + P^{ext}\hat\Omega,$$

where $\hat\Omega$ is a virtual angular velocity, P^{int} and P^{ext} are respectively the internal percussion and the external percussion. The Principle gives the equation of motion

$$J(\Omega^+ - \Omega^-) = -P^{int} + P^{ext}.$$

We assume no external percussion, and so get

$$J(\Omega^+ - \Omega^-) = -P^{int}. \tag{5}$$

3.2. **Constitutive law.** In order to be consistent with the non-smooth versions of the energy balance and the second law of thermodynamics [6, 9], the constitutive assumption on P^{int} has to satisfy the constitutive condition:

$$P^{int}\,\frac{\Omega^+ + \Omega^-}{2} \geq 0. \tag{6}$$

If Φ is a pseudopotential of dissipation, a theorem of convex analysis [7, 8] asserts that if

$$P^{int} \in \partial\Phi\left(\frac{\Omega^+ + \Omega^-}{2}\right), \tag{7}$$

then (6) is satisfied. We also have to choose Φ such that the *impenetrability condition* – which, in the case of $\vartheta = \pi$, reads $\Omega^+ \leq 0$ – is satisfied [9]. Thus, we take

$$\Phi\left(\frac{\Omega^+ + \Omega^-}{2}\right) = \hat{k}\left(\frac{\Omega^+ + \Omega^-}{2}\right)^2 + I_-\left(\frac{\Omega^+ + \Omega^-}{2} - \frac{\Omega^-}{2}\right),$$

where $\hat{k}$ is the dissipation constant in the collision[3]. It is easy to check that two of the three properties characterizing a pseudopotential of dissipation, namely, $\Phi \geq 0$ and Φ convex, are satisfied; the last one, $\Phi(0) = 0$, is satisfied because $I_-\left(-\frac{\Omega^-}{2}\right) = 0$, since $\Omega^- \geq 0$ for $\vartheta = \pi$. Hence, (7) becomes

$$P^{int} \in \hat{k}(\Omega^+ + \Omega^-) + \partial I_-(\Omega^+)$$

and the equation of motion (5) gives, with the previous constitutive law:

$$(J - \hat{k})\Omega^- \in (J + \hat{k})\Omega^+ + \partial I_-(\Omega^+).$$

We suppose to know Ω^- and want to compute Ω^+. We distinguish between two cases:

- $J - \hat{k} \geq 0 \Longrightarrow \Omega^+ = 0$ (the forearm does not bounce);
- $J - \hat{k} < 0 \Longrightarrow \Omega^+ = \dfrac{J - \hat{k}}{J + \hat{k}}\,\Omega^-$ (the forearm bounces).

We can easily repeat all these arguments for a collision when $\vartheta = 0$ and, since the impenetrability condition becomes $\Omega^+ \geq 0$, we get the following equation of motion:

$$(J - \hat{k})\Omega^- \in (J + \hat{k})\Omega^+ + \partial I_+(\Omega^+),$$

I_+ being the indicator function of $[0, +\infty)$. In this situation, we also have $\Omega^- \leq 0$, thus:

- $J - \hat{k} \leq 0 \Longrightarrow \Omega^+ = \dfrac{J - \hat{k}}{J + \hat{k}}\,\Omega^-$ (the forearm bounces);
- $J - \hat{k} > 0 \Longrightarrow \Omega^+ = 0$ (the forearm does not bounce).

[3] In fact, $I_-\left(\frac{\Omega^+ + \Omega^-}{2} - \frac{\Omega^-}{2}\right) = I_-\left(\frac{\Omega^+}{2}\right) = I_-(\Omega^+)$, which gives the impenetrability condition.

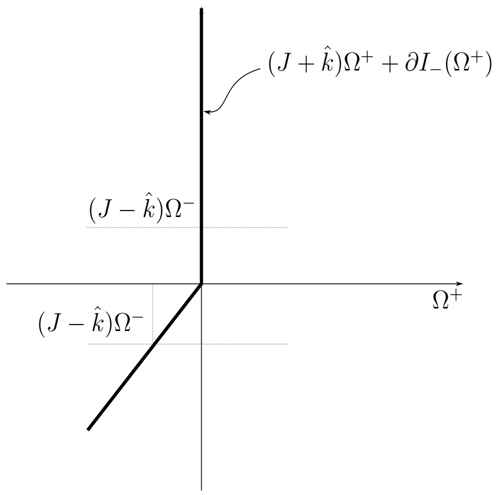

FIGURE 2. Collision for $\vartheta = \pi$.

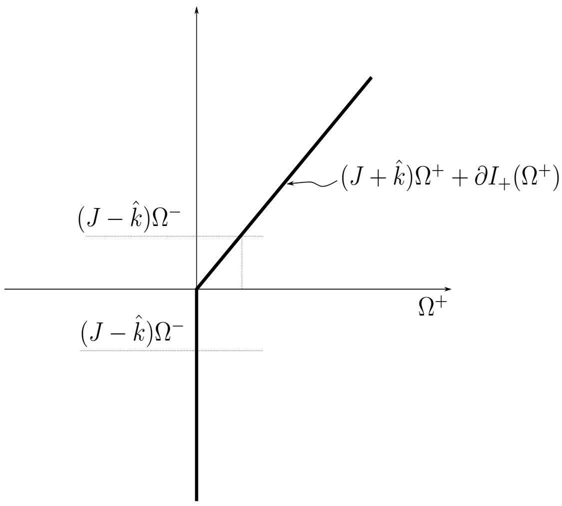

FIGURE 3. Collision for $\vartheta = 0$.

4. Numerical results

In this section we provide some results of the numerical simulation of equations (4). The system has been solved with the finite-difference method. In all the following simulations, two of the initial conditions are always the same: $\vartheta(0) = 0$ and $\beta(0) = 1$ (at the beginning of the process, the forearm lays on the arm and the articulation is sound); on the contrary, we change the initial angular velocity $\dot{\vartheta}(0)$.

4.1. **Numerical scheme.** The numerical method has been chosen simple, in order to focus on the mechanical problem. Thus we have chosen an event-driven method [10]. For the mathematical analysis of the problem, we refer to [11, 12], where equations with the same structure are investigated. The solutions are either bounded variation functions of time or special bounded variation functions of time.

Let $T > 0$ and $\mathcal{T} = [0, T]$ be the observation time horizon of the system. We split $\mathcal{T}$ into N smaller time intervals, whence the time step $\Delta t = \frac{T}{N}$. Let $t \mapsto \eta(t)$ be a generic function. We set

$$\eta_k = \eta(k\Delta t) \quad (k = 0, \dots, N).$$

Thus, the first and second derivatives of η are approximated as follows:

$$\dot{\eta}(t) \simeq \frac{\eta_{k+1} - \eta_k}{\Delta t}, \quad \ddot{\eta}(t) \simeq \frac{\eta_{k+1} - 2\eta_k + \eta_{k-1}}{\Delta t^2}.$$

Therefore, assuming the constraints of the problem are satisfied ($B^r = C^r \equiv 0$), the equations of motion (4) become

$$\tag{8} \begin{cases} J \dfrac{\vartheta_{k+1} - 2\vartheta_k + \vartheta_{k-1}}{\Delta t^2} + \nu \dfrac{\vartheta_{k+1} - \vartheta_k}{\Delta t} + k\beta_k\vartheta_{k+1} = C_k \\ c \dfrac{\beta_{k+1} - \beta_k}{\Delta t} = w - \dfrac{1}{2}k\vartheta_{k+1}^2 \\ \vartheta_0 = 0, \;\; \beta_0 = 1. \end{cases}$$

where the subscript k in the external couple C stresses the fact that this load may depend on time. Note that, for $k = 0$, a term containing ϑ_{-1} results from $(8)_1$. We can compute the value of ϑ_{-1} by taking into account that

$$\dot{\vartheta}(0) \simeq \frac{\vartheta_0 - \vartheta_{-1}}{\Delta t} = -\frac{\vartheta_{-1}}{\Delta t} \Longrightarrow \vartheta_{-1} \simeq -\dot{\vartheta}(0)\Delta t,$$

where $\dot{\vartheta}(0)$, the initial angular velocity, is known.

At each iteration, the system of algebraic equations (8) allows to compute the values of ϑ_{k+1} and β_{k+1}, based on the known values of ϑ_{k-1}, ϑ_k and β_k. The iteration index k is increased by one after every computation of ϑ_{k+1} and β_{k+1}.

We take account of the problem constraints as follows:

(*i*) if $\vartheta_{k+1} > \pi$ ($\vartheta_{k+1} < 0$), set $\vartheta_{k+1} = \pi$ ($\vartheta_{k+1} = 0$) and compute the angular velocity before the collision,

$$\Omega^- = \frac{\vartheta_k - \vartheta_{k-1}}{\Delta t}.$$

Then, compute the angular velocity after the collision Ω^+ by using the formulae set forth in section 3, according to whether $J - \hat{k} \geq 0$ or $J - \hat{k} < 0$. The value of ϑ_{k+2} is consequently given by

$$\tag{9} \Omega^+ = \frac{\vartheta_{k+2} - \vartheta_{k+1}}{\Delta t} \Longrightarrow \vartheta_{k+2} = \vartheta_{k+1} + \Omega^+\Delta t.$$

When a collision occurs, after computing ϑ_{k+2} by using (9), the iteration index has to be increased by one further on, in order for the value of ϑ_{k+2} given by (9) not to be overwritten by the value of ϑ_{k+2} given by $(8)_1$, as it would be computed in the next iteration;

(*ii*) if $\beta_{k+1} < 0$ ($\beta_{k+1} > 1$), set $\beta_{k+1} = 0$ ($\beta_{k+1} = 1$);

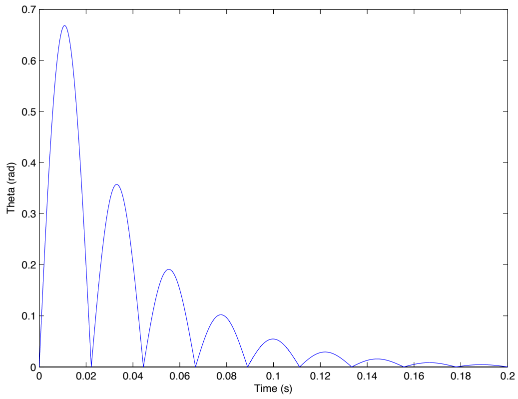

FIGURE 4. $t \mapsto \vartheta(t)$ with $\dot{\vartheta}_0 = 100\,rad\,s^{-1}$, $J = 5\,kg\,m^2$, $\nu = 50\,Nm\,s$, $k = 10^5\,Nm$, $C = 0$, $w = 10^{10}\,Nm$, $c = 0.1\,Nm\,s$, $\hat{k} = 20\,kg\,m^2$. The forearm repeatedly collides, with smaller and smaller oscillations, only for $\vartheta = 0$ and then goes to rest.

(*iii*) if $\beta_{k+1} > \beta_k$, set $\beta_{k+1} = \beta_k$.

Remark 3. *In order to capture as many collisions as possible, the timestep Δt (i.e., the number of smaller time intervals N) has to be chosen properly. In all of our simulations, we chose $N = 10^4$ and, in most cases, $T = 0.2\,s$, whence $\Delta t = 20\,\mu s$.*

4.2. **A basic example.** We choose the evolution with data $J = 5\,kg\,m^2$, $\nu = 50\,Nm\,s$, $k = 10^5\,Nm$, $C = 0$, $w = 10^{10}\,Nm$, $c = 0.1\,Nm\,s$, $\hat{k} = 20\,kg\,m^2$ as a reference to illustrate the effect of the physical parameters. For this basic example, we choose two initial angular velocities. We get the graph in fig. 4 with $\dot{\vartheta}_0 = 100\,rad\,s^{-1}$ and the graph in fig. 5 with $\dot{\vartheta}_0 = 500\,rad\,s^{-1}$. In the former case, we have collisions only when $\vartheta = 0$ and no damage, because the initial angular velocity is not sufficient for the forearm to reach $\vartheta = \pi$ and the cohesion energy w, which may be regarded as the strength of the articulation, is five orders greater than its stiffness; in the latter one, we still have no damage, but we also have one collision at $\vartheta = \pi$, and then repeated collisions at $\vartheta = 0$ until the system goes to rest.

4.3. **Influence of the mass moment of inertia.** If the mass moment of inertia is increased ($J = 30\,kg\,m^2$) and all the other constants remain unchanged, we get the evolution of ϑ shown in fig. 6 for $\dot{\vartheta}_0 = 100\,rad\,s^{-1}$ and the one shown in fig. 7 for $\dot{\vartheta}_0 = 500\,rad\,s^{-1}$; in both cases, there is still no damage. In the former case, the forearm does not reach $\vartheta = \pi$ and then goes back to $\vartheta = 0$ because of the effect of the hair spring, and after only one collision goes to rest. In the latter one, the forearm reaches $\vartheta = \pi$ and goes back after a collision.

4.4. **Influence of the cohesion energy and the damage viscosity.** By setting again $J = 5\,kg\,m^2$, decreasing the cohesion energy ($w = 4.5 \cdot 10^5\,Nm$), slightly increasing the stiffness and significantly increasing the damage viscosity ($k = 1.03 \cdot 10^5\,Nm$, $c = 100\,Nm\,s$),

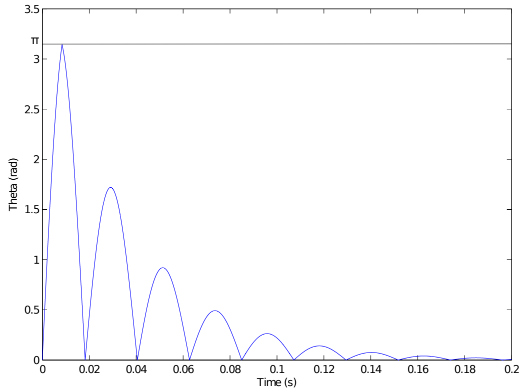

FIGURE 5. $t \mapsto \vartheta(t)$ with $\dot{\vartheta}_0 = 500\,rad\,s^{-1}$, $J = 5\,kg\,m^2$, $\nu = 50\,Nm\,s$, $k = 10^5\,Nm$, $C = 0$, $w = 10^{10}\,Nm$, $c = 0.1\,Nm\,s$, $\hat{k} = 20\,kg\,m^2$. The forearm collides only once for $\vartheta = \pi$ and the other collisions are for $\vartheta = 0$, and then it goes progressively to rest.

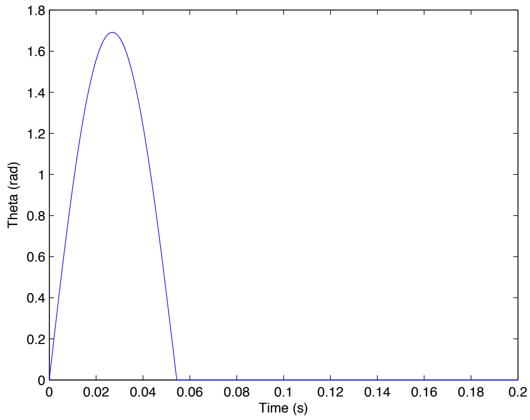

FIGURE 6. $t \mapsto \vartheta(t)$ with $\dot{\vartheta}_0 = 100\,rad\,s^{-1}$, $J = 30\,kg\,m^2$, $\nu = 50\,Nm\,s$, $k = 10^5\,Nm$, $C = 0$, $w = 10^{10}\,Nm$, $c = 0.1\,Nm\,s$, $\hat{k} = 20\,kg\,m^2$. Due to the effects of J and k, the initial velocity is not sufficient for the forearm to reach $\vartheta = \pi$ and once ϑ reaches its maximum, it goes back to rest.

we get the same evolution as shown in fig. 4 for $\dot{\vartheta}_0 = 100\,rad\,s^{-1}$, and the one shown in fig. 8 for $\dot{\vartheta}_0 = 500\,rad\,s^{-1}$. It is quite interesting to note that, while in the former case we still have no damage, in the latter the damage evolves as shown in fig. 9. In the former case, we have no collision at $\vartheta = \pi$ and no damage; in the latter, we have one collision at $\vartheta = \pi$ which occurs at time $t^* \in [0, 0.02\,s]$ and damage starts as soon as $\vartheta > \sqrt{2w/k}$, decreasing rapidly, until it reaches a constant value $\overline{\beta} \in [0.15, 0.2]$.

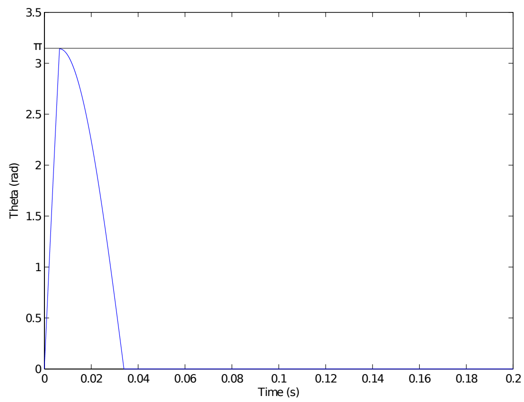

FIGURE 7. $t \mapsto \vartheta(t)$ with $\dot{\vartheta}_0 = 500\, rad\, s^{-1}$, $J = 30\, kg\, m^2$, $\nu = 50\, Nm\, s$, $k = 10^5\, Nm$, $C = 0$, $w = 10^{10}\, Nm$, $c = 0.1\, Nm\, s$, $\hat{k} = 20\, kg\, m^2$. Having increased the initial angular velocity, the forearm reaches $\vartheta = \pi$, collides and then goes back to rest, stopping after one collision for $\vartheta = 0$.

4.5. **Influence of the cohesion energy, the elastic stiffness, the dissipation and the mass moment of inertia.** When the cohesion energy is remarkably decreased ($w = 1\, Nm$), together with the dissipation in the collision and the stiffness of the spring ($\hat{k} = 1\, kg\, m^2$, $k = 20\, Nm$), and the mass moment of inertia is significantly increased ($J = 10^5\, kg\, m^2$), with $C = 0$, $c = 0.1\, Nm\, s$ and $\dot{\vartheta}_0 = 100\, rad\, s^{-1}$ we obtain the graphs shown in figs. 10 and 11. If we increase the initial angular velocity to $\dot{\vartheta}_0 = 500\, rad\, s^{-1}$ we obtain results which are not so different, apart from the slope of the damage after it starts and of ϑ before reaching π. Because of the high value of the mass moment of inertia and the low value of the stiffness k, when the forearm reaches $\vartheta = \pi$ it collides and does not bounce, but goes back very slowly to $\vartheta = 0$; damage begins before the collision.

4.6. **Influence of the external torque.** Let us now examine the cases in which an external torque is applied on the forearm. We shall distinguish between two subcases.

4.6.1. ***C is constant.*** To emphasize the influence of a constant external torque, we have slightly changed the mass moment of inertia ($J = 1\, kg\, m^2$), the motion viscosity ($\nu = 3\, Nm\, s$), the elastic stiffness ($k = 40\, Nm$) and the cohesion energy ($w = 100\, Nm$). The damage viscosity and the dissipation remain $c = 0.1\, Nm\, s$, $\hat{k} = 20\, kg\, m^2$ and the external torque is $C = 10^3\, Nm$. With this set of data, we get the graphs shown in figs. 12 and 13 for $\dot{\vartheta}_0 = 100\, rad\, s^{-1}$ and the ones shown in figs. 14 and 15 for $\dot{\vartheta}_0 = 10^3\, rad\, s^{-1}$; when $\dot{\vartheta}_0 = 500\, rad\, s^{-1}$, the results are not very different (at least from the point of view of damage) from the case in which $\dot{\vartheta}_0 = 100\, rad\, s^{-1}$. In the former case, we have only one collision at $\vartheta = 0$ and then many collisions at $\vartheta = \pi$ with more and more reduced oscillations; damage starts before the first collision at $\vartheta = \pi$ occurs, and decreases very rapidly to 0. In the latter case, we have several collisions when either $\vartheta = 0$ or $\vartheta = \pi$;

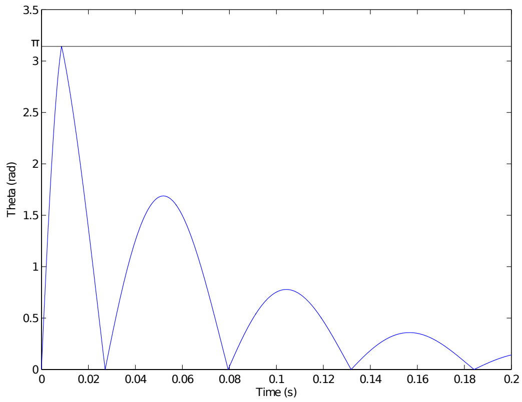

FIGURE 8. $t \mapsto \vartheta(t)$ with $\dot{\vartheta}_0 = 500\,rad\,s^{-1}$, $J = 5\,kg\,m^2$, $\nu = 50\,Nm\,s$, $k = 1.03 \cdot 10^5\,Nm$, $C = 0$, $w = 4.5 \cdot 10^5\,Nm$, $c = 100\,Nm\,s$, $\hat{k} = 20\,kg\,m^2$. The forearm repeatedly collides, but it tends to reach $\vartheta = 0$ not as rapidly as in the case of fig. 5 because of the damage viscosity.

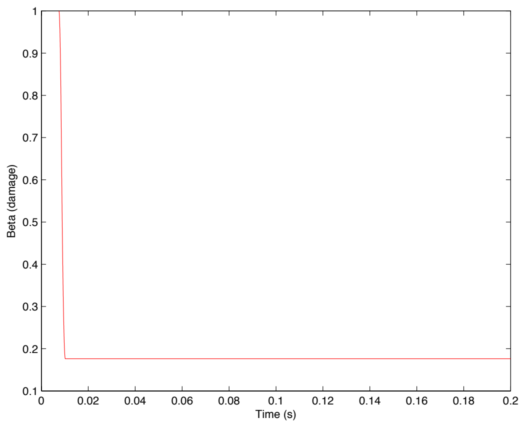

FIGURE 9. $t \mapsto \beta(t)$ with $\dot{\vartheta}_0 = 500\,rad\,s^{-1}$, $J = 5\,kg\,m^2$, $\nu = 50\,Nm\,s$, $k = 1.03 \cdot 10^5\,Nm$, $C = 0$, $w = 4.5 \cdot 10^5\,Nm$, $c = 100\,Nm\,s$, $\hat{k} = 20\,kg\,m^2$. Damage starts as soon as ϑ is large enough and it decreases very rapidly till reaching a constant value. Here, the role of the initial angular velocity is important: indeed, we get no damage with $\dot{\vartheta}_0 = 100\,rad\,s^{-1}$.

damage starts after a very short time from the beginning of the process, it decreases very rapidly to a value $\beta^* \in [0.1, 0.15]$ and, after remaining constant and equal to β^* in a very short time interval $\tau \subset [0, 0.01\,s]$, it goes to 0.

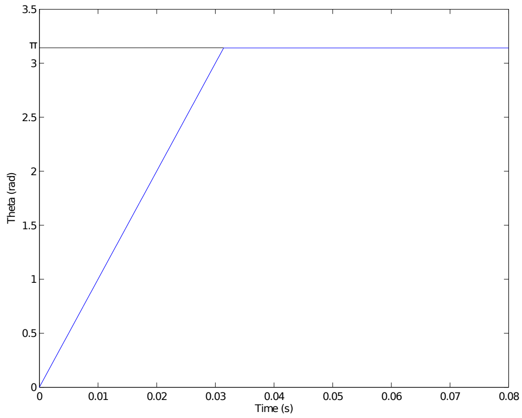

FIGURE 10. $t \mapsto \vartheta(t)$ with $\dot{\vartheta}_0 = 100\, rad\, s^{-1}$, $J = 10^5\, kg\, m^2$, $\nu = 50\, Nm\, s$, $k = 20\, Nm$, $C = 0$, $w = 1\, Nm$, $c = 0.1\, Nm\, s$, $\hat{k} = 1\, kg\, m^2$. Due to the large initial velocity, the forearm reaches $\vartheta = \pi$ and collides without bouncing, but due to the large mass moment of inertia it goes back very slowly to its equilibrium position $\vartheta = 0$.

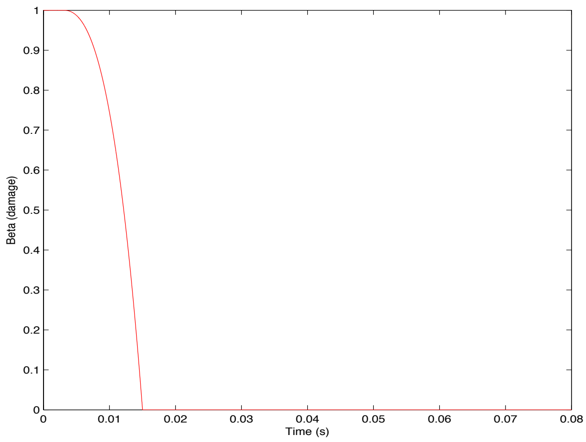

FIGURE 11. $t \mapsto \beta(t)$ with $\dot{\vartheta}_0 = 100\, rad\, s^{-1}$, $J = 10^5\, kg\, m^2$, $\nu = 50\, Nm\, s$, $k = 20\, Nm$, $C = 0$, $w = 1\, Nm$, $c = 0.1\, Nm\, s$, $\hat{k} = 1\, kg\, m^2$. Damage starts before collision occurs.

4.6.2. ***C depends on time.*** We have noted that, for some special dependences of the external torque on time, the results previously obtained are remarkably changed. If we choose $C(t) = (t+3)^{10}$ (neglecting physical dimensions) and use the remaining set of data as identical to the one used to get the evolutions of ϑ and β respectively visualized in figs. 8 and 9, we get the evolutions visualized in figs. 16 and 17. Choosing dependences on time

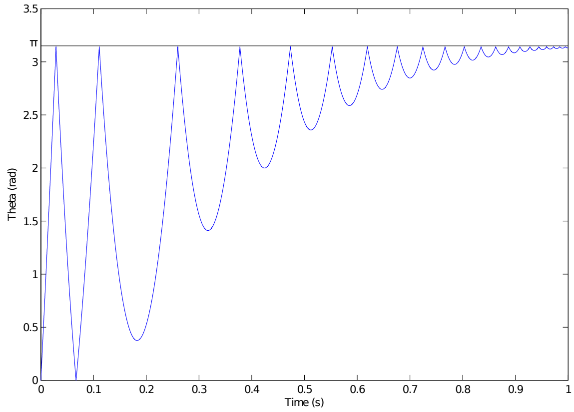

FIGURE 12. $t \mapsto \vartheta(t)$ with $\dot{\vartheta}_0 = 100\,rad\,s^{-1}$, $J = 1\,kg\,m^2$, $\nu = 3\,Nm\,s$, $k = 40\,Nm$, $w = 100\,Nm$, $c = 0.1\,Nm\,s$, $\hat{k} = 20\,kg\,m^2$ and $C = 10^3\,Nm$. The effect of the external torque is to make the system to reach $\vartheta = \pi$ and then to rest after repeated collisions.

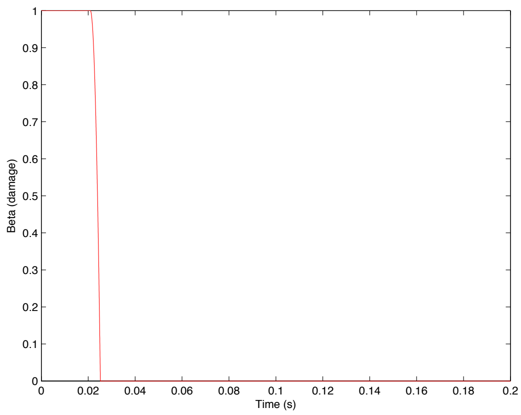

FIGURE 13. $t \mapsto \beta(t)$ with $\dot{\vartheta}_0 = 100\,rad\,s^{-1}$, $J = 1\,kg\,m^2$, $\nu = 3\,Nm\,s$, $k = 40\,Nm$, $w = 100\,Nm$, $c = 0.1\,Nm\,s$, $\hat{k} = 20\,kg\,m^2$ and $C = 10^3\,Nm$. Damage starts before collision occurs, decreasing very rapidly to 0.

of C such as t, t^2, $\log(t+1)$, $\sin t$, e^t, does not lead to behaviours significantly different from the ones represented in figs. 8 and 9.

5. Conclusions

The elbow motion predictive theory is based on discontinuum and continuum mechanics. It is a schematic but realistic model of the evolution of an elbow which may lose its elasticity

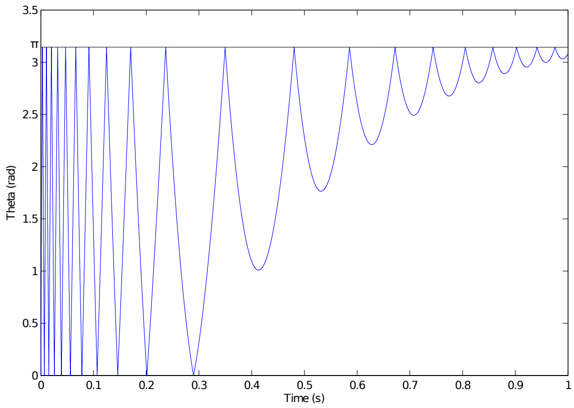

FIGURE 14. $t \mapsto \vartheta(t)$ with $\dot{\vartheta}_0 = 10^3\, rad\, s^{-1}$, $J = 1\, kg\, m^2$, $\nu = 3\, Nm\, s$, $k = 40\, Nm$, $w = 100\, Nm$, $c = 0.1\, Nm\, s$, $\hat{k} = 20\, kg\, m^2$ and $C = 10^3\, Nm$. If the initial angular velocity is increased by one order of magnitude, the number of collisions for $\vartheta = 0$ is remarkably increased.

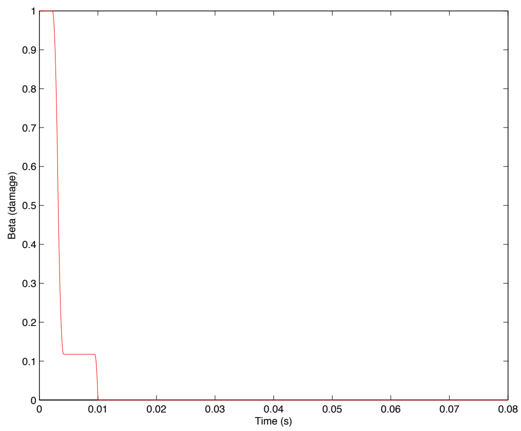

FIGURE 15. $t \mapsto \beta(t)$ with $\dot{\vartheta}_0 = 10^3\, rad\, s^{-1}$, $J = 1\, kg\, m^2$, $\nu = 3\, Nm\, s$, $k = 40\, Nm$, $w = 100\, Nm$, $c = 0.1\, Nm\, s$, $\hat{k} = 20\, kg\, m^2$ and $C = 10^3\, Nm$. If the initial angular velocity is increased by one order of magnitude, damage evolves decreasing very rapidly after a short time interval from the beginning of the process, remaining constant for another short time interval and then going to 0.

due to external mechanical damaging actions, for instance in the tennis elbow pathology. Few parameters are involved. The model, which is coherent from the mechanical, numerical and mathematical point of view (it can be proved that its equations have a unique solution), may be sophisticated and upgraded in many ways to fit with every day behavior.

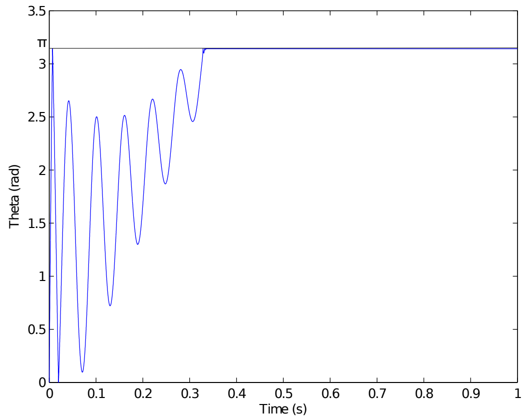

FIGURE 16. $t \mapsto \vartheta(t)$ with $\dot{\vartheta}_0 = 500\, rad\, s^{-1}$, $J = 5\, kg\, m^2$, $\nu = 50\, Nm\, s$, $k = 1.03 \cdot 10^5\, Nm$, $w = 4.5 \cdot 10^5\, Nm$, $c = 100\, Nm\, s$, $\hat{k} = 20\, kg\, m^2$, $C(t) = (t+3)^{10}$. The time dependence of the external torque makes the forearm to collide one time at $\vartheta = \pi$ and at $\vartheta = 0$; after these two collisions, it makes various smooth oscillations, with $0 < \vartheta < \pi$, till it reaches again $\vartheta = \pi$, collides again and remains at this position due to the effect of the large torque.

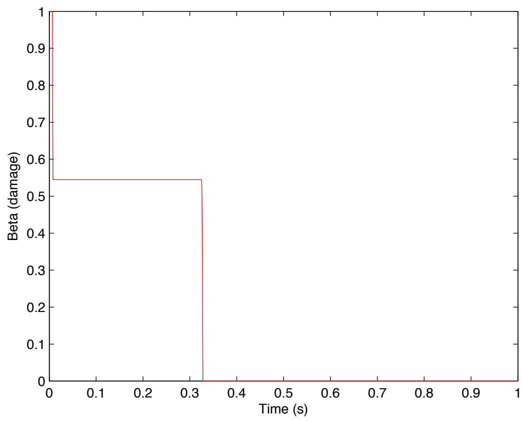

FIGURE 17. $t \mapsto \beta(t)$ with $\dot{\vartheta}_0 = 500\, rad\, s^{-1}$, $J = 5\, kg\, m^2$, $\nu = 50\, Nm\, s$, $k = 1.03 \cdot 10^5\, Nm$, $w = 4.5 \cdot 10^5\, Nm$, $c = 100\, Nm\, s$, $\hat{k} = 20\, kg\, m^2$, $C(t) = (t+3)^{10}$. We have obtained an evolution of damage which is analogous to the one visualized in fig. 15, but the time interval in which β remains constant is much larger than the one of fig. 15.

REFERENCES

[1] M. A. Lemay and P. Crago, A dynamic model for simulating movements of the elbow, forearm, and wrist, J. Biomechanics, Vol. 29, No. 10, pp. 1319-1330, 1996.

[2] S. Riek, A. E. Chapman, T. Milner, A simulation of muscle force and internal kinematics of extensor carpi radialis brevis during backhand tennis stroke: implications for injury, Clinical Biomechanics 14 (1999) 477-483.
[3] E. J. van Zuylen, A. van Velzen and J. J. Denier van der Gon, A biomechanical model for flexion torques of human arm muscles as a function of elbow angle, J. Biomechanics Vol. 21, No. 3, pp. 183-190, 1988.
[4] M. Frémond, B. Nedjar, 1996, Damage, gradient of damage and principle of virtual power, Int. J. Solids Struct., 33, 8, 1083-1103.
[5] N. Pede, P. Podio-Guidugli, G. Tomassetti, 2006, Balancing the force that drives the peeling of an adhesive tape, Il Nuovo Cimento, 121 B, 5, 531-543.
[6] M. Frémond, *Non-smooth thermomechanics*, Springer-Verlag, Berlin 2002.
[7] J. J. Moreau, *Fonctionnelles convexes*, Dipartimento di Ingegneria Civile, Università Tor Vergata, Roma, 2003, ISBN 978-88-6296-001-4 and Séminaire sur les équations aux dérivées partielles, Collège de France, Paris 1966.
[8] I. Ekeland, R. Temam, *Analyse convexe et problèmes variationnels*, Dunod-Gauthier-Villars 1974.
[9] M. Frémond, *Collisions*, Dipartimento di Ingegneria Civile dell'Università di Roma Tor Vergata, ISBN 978-88-6296-000-7.1, 2007.
[10] M. Jean, Numerical Simulation of Granular Materials, Chapter 4 in *Micromechanics of Granular Materials*, B. Cambou, M. Jean, F. Radjaï editors, John Wiley and Sons, 2010, DOI 10.1002/9780470611616.ch4.
[11] C. Cholet, Chocs de solides rigides, PhD thesis, Université Pierre et Marie Curie, Paris, 1998.
[12] C. Cholet, Collision d'un point et d'un plan, C.R. Acad. Sci., Paris 328, Serie I, 445-458, 1999, DOI 10.1016/S0764-4442(99)80189-X.

This paper is dedicated to Gianpietro Del Piero and Michel Jean, mechanicians who may have experimented elbow or knee troubles.

(Francesco Bonaldi) Facoltà di Ingegneria, Università degli Studi di Roma Tor Vergata, Via del Politecnico, 00100 Roma, Italy

(Michel Frémond) Dipartimento di Ingegneria Civile, Facoltà di Ingegneria, Università degli Studi di Roma Tor Vergata, Via del Politecnico, 00100 Roma, Italy